

Electrostatic Contribution to Line Tension in a Wedge-Shaped Contact Region

Kwan Hyoung Kang,^{*,†} In Seok Kang,[‡] and Choung Mook Lee[†]

Department of Mechanical Engineering and Department of Chemical Engineering,
Pohang University of Science and Technology, San 31, Hyoja-dong,
Pohang 790-784, Republic of Korea

Received March 28, 2003. In Final Form: June 13, 2003

In the wetting problems of very small scales, such as in nanotubes and nanoparticles, the contribution of line tension potentially becomes significant. In contrast to the molecular contribution, there rarely exists any literature that systematically considers the electrical contribution to the line tension in wetting. In this paper, the electrical double layer around a wedge-shaped confinement (which represents the region of the three-phase contact of an electrolyte droplet on a charged, or ionizable, substrate) is analyzed. An exact analytical solution for the linearized Poisson–Boltzmann equation is obtained for both the constant surface charge and the constant surface potential conditions. Comprehensive analytical formulas of the line tension are derived. An equation for predicting the contact angle is also shown, considering the dependence of the electrostatic line tension on the contact angle. It is exhibited that the line tension can have either a positive or a negative value depending on the sign of the surface charge density. It is demonstrated that the magnitude of the line tension is comparable or (potentially) greater than that of the molecular contribution. To corroborate the results of the linear theory, the nonlinear Poisson–Boltzmann equation is solved numerically. The results of the nonlinear theory show reasonable agreement with those of the linear theory.

Introduction

The line tension (τ) is a measure of the excess free energy per unit length (having the dimension of joule per meter, or newton) of the contact line at the boundary between three bulk phases. It is a one-dimensional analogue of the surface tension and represents the edge effect in wetting of a liquid layer (film or droplet) sitting on a substrate. The theoretical prediction of the line tension indicates that it has very small values ranging from 10^{-12} to 10^{-10} N (see, e.g., refs 1 and 2). However, the line-tension correction term appears in Young's equation in the form of τ/R , where R represents typically the base (contact) radius of a droplet. Therefore, its effect becomes significant as the droplet size gets smaller, such as for interfacial problems of fine colloidal particles, droplets, and bubbles.

The line tension, thus, plays an important role in determining the contact angle of a microscopic droplet, the nucleation behavior of a droplet on a surface, the dynamics of contact-line spreading, and the attachment of solid particles to a fluid interface.^{1–4} Furthermore, the recent shift in interest to much smaller scales increases the concern for the line-tension effect. This includes the wetting problem of a nanotube,^{5–9} the contact-line evolution in patterned substrates,¹⁰ and the wetting transition of nanoparticles at a fluid interface.^{11,12} Although there is a certain limit in the macroscopic description of wetting in very small scales, the extension of the macroscopic

description employing the line tension is still a useful alternative to the molecular approach.¹³

The Coulombic interaction is a key factor in the wetting of electrolyte liquid on a charged (or ionizable) surface.^{14–17} The line tension originates from the local change of the interactions near the three-phase contact line (such as of van der Waals, electrostatic, etc.), with respect to those of the bulk region, due to the existence of the third phase. Like what the van der Waals and other interactions do to what we call the molecular line tension, the electrostatic interaction will be perturbed near the three-phase contact line (TCL) and will certainly contribute to the line tension.

In contrast to the molecular contribution, little attention has been paid to the electrostatic contribution to the line tension in wetting problems. Among them, Denkov et al.¹⁸ have considered the case of the two flocculating droplets. They obtained the line tension (under the Derjaguin approximation) including the van der Waals interaction, the electrostatic interaction, and the deformation of the

* To whom correspondence should be addressed. E-mail: khkang@postech.edu.

[†] Department of Mechanical Engineering, Pohang University of Science and Technology.

[‡] Department of Chemical Engineering, Pohang University of Science and Technology.

(1) Wang, J. Y.; Betelu, S.; Law, B. M. *Phys. Rev. E* **2001**, *63*, 031601.

(2) Drellich, J. *Colloids Surf.* **1996**, *116*, 43–54.

(3) Ivanov, I. B.; Kralchevsky, P. A.; Nikolov, A. D. *J. Colloid Interface Sci.* **1986**, *112*, 97–107.

(4) Aveyard, R.; Clint, J. H.; Nees, D. *Colloid Polym. Sci.* **2000**, *278*, 155–163.

(5) Dujardin, E.; Ebbesen, T. W.; Hiura, H.; Tanigaki, K. *Science* **1994**, *265*, 1850–1852.

(6) Ugarte, D.; Châtelain, A.; de Heer, W. A. *Science* **1996**, *274*, 1897–1899.

(7) Ebbesen, T. W. *J. Phys. Chem. Solids* **1996**, *57*, 951–955.

(8) Bauer, C.; Dietrich, S. *Phys. Rev. E* **2000**, *62*, 2428–2438.

(9) Werder, T.; Walther, J. H.; Jaffe, R. L.; Halicioglu, T.; Koumoutsakos, P. *J. Phys. Chem. B* **2003**, *107*, 1345–1352.

(10) Buehrle, J.; Herminghaus, S.; Mugele, F. *Langmuir* **2002**, *18*, 9771–9777.

(11) Bresme, F.; Quirke, N. *Phys. Rev. Lett.* **1998**, *80*, 3791–3794.

(12) Bresme, F.; Quirke, N. *Phys. Chem. Chem. Phys.* **1999**, *1*, 2149–2155.

(13) Powell, C.; Fenwick, N.; Bresme, F.; Quirke, N. *Colloids Surf.* **2002**, *206*, 241–251.

(14) Digilov, R. *Langmuir* **2000**, *16*, 6719–6723.

(15) Chou, T. *Phys. Rev. Lett.* **2001**, *87*, 106101.

(16) Kang, K. H.; Kang, I. S.; Lee, C. M. *Langmuir* **2003**, *19*, 5407–5412.

(17) Kang, K. H.; Kang, I. S.; Lee, C. M. *Langmuir* **2003**, *19*, 6881–6887.

(18) Denkov, N. D.; Petsev, D. N.; Danov, K. D. *J. Colloid Interface Sci.* **1995**, *176*, 189–200.

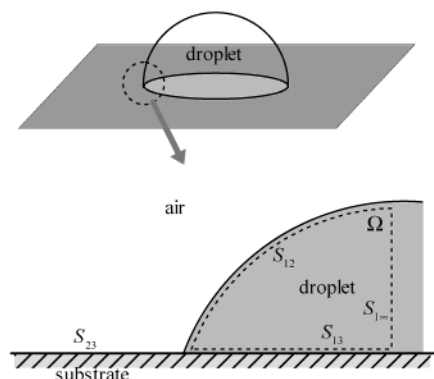


Figure 1. Coordinate system and definition of variables.

liquid surface. To our knowledge, there exist only two recent theoretical investigations of Digilov¹⁴ and Chou¹⁵ that are concerned with the electrostatic line tension for systems similar to those of the present interest. The work of Digilov¹⁴ is concerned with the role of the line tension in wetting but without an assessment of the magnitude of the line tension. Chou¹⁵ briefly discussed that the line tension on a charged surface should be $\sigma/(\epsilon\kappa^2)$ times a factor dependent on the contact angle, where σ is the surface charge density, ϵ is the electric permittivity, and κ is the inverse Debye length. However, he did not provide any information on the detailed functional dependence of the line tension on the contact angle. This motivates the present work of the quantitative assessment of the electrostatic contribution to the line tension.

In the present paper, we provide analytical results for predicting the line tension of electrostatic origin in the case of a simple geometry. For this, the linearized Poisson–Boltzmann equation is solved analytically for a wedge-shaped geometry, which is a representative model of the edge of a droplet sitting on an ionizable substrate. The analytical formulas of the line tension and its gradient with respect to the contact angle are obtained in eqs 24, 25, 28, and 29 for the constant charge (CC) and the constant potential (CP) cases, respectively. The nonlinear Poisson–Boltzmann equation is also solved numerically, and the results show reasonable agreement with those of the linear theory. It is demonstrated that the magnitude of the line tension is comparable or even greater than that of the molecular contribution. Also shown is that, in the CC case, the sign of the line tension can be either positive or negative depending on the value of the surface charge density.

The present investigation is not intended to compare with existing experimental data or to explain the well-known large discrepancy between predictions and experiments.^{1,2,4,10,19–20} Unfortunately, because there is no means of measuring the electrical contribution to the line tension separately, a verification of our results cannot be performed. Nevertheless, the present work is meaningful in that it provides an analytical modeling of the line tension under the charge-related wetting configurations and will become a basis for further investigations on the electrically induced line-tension effect.

Free Energy of the System

We consider a droplet in stable equilibrium on a solid substrate, submerged in another liquid or air. For most of the practically important circumstances, however, air is the surrounding fluid. So, we limit our attention to the case of air as the surrounding fluid. A cross section of the droplet shown in Figure 1 can be imagined to continue normal to the page. We introduce a control surface $\Sigma =$

$S_{12} \cup S_{13} \cup S_{1\infty}$, which encloses the edge region of the droplet (Ω). Hereafter, the indices 1, 2, and 3 will denote the variables associated with the droplet, the air, and the substrate, respectively. The double indices in S_{jk} denote the surface in the j th medium facing the k th medium.

The total free energy of the system (G_{tot}) can be represented as a sum of the mechanical (G_{mech}) and the electrochemical (G) parts. The electrochemical part can be further decomposed to electrostatic (G_{el}) and chemical parts (G_{chem}); that is, $G = G_{\text{el}} + G_{\text{chem}}$. Then, neglecting the gravitational effect and assuming the interfacial tension on a given interface is a constant value, the variable part of G_{tot} can be written as^{21,22}

$$\begin{aligned} G_{\text{tot}} &= G_{\text{mech}} + G_{\text{el}} + G_{\text{chem}} \\ &= \gamma_{12}A_{12} + (\gamma_{13} - \gamma_{23})A_{13} + \int_{\Sigma} dS \int_0^{\sigma} \varphi_s(\sigma) d\sigma + \\ &\quad \int_{\Sigma} dS \sum_m \int_0^{\Gamma_m} (\bar{\mu}_m^s - \mu_m^b) d\Gamma_m \end{aligned} \quad (1)$$

where the first two terms, the third term, and the fourth term correspond to G_{mech} , G_{el} , and G_{chem} , respectively. Here, γ_{jk} and A_{jk} denote the interfacial tensions and the surface areas, φ_s is the electrostatic potential at the surface, and Γ_m is the amount of the m th ionic species adsorbed per unit surface area, which is related with the surface charge density as $\sigma = \sum_m z_m e \Gamma_m$ (where z_m is the valence of m th ionic species and e is the electronic charge). $\bar{\mu}_m^s$ and μ_m^b are the chemical potentials of m th ionic species at the surface and in the bulk liquid, and $\bar{\mu}_m^s$ is related with the electrochemical potential as

$$\mu_m^s = \bar{\mu}_m^s + z_m e \varphi_s \quad (2)$$

Note that the interfacial tension of a charged interface is modified by the contributions from the adsorption layer and the diffuse electric double layer (see, e.g., refs 23–24). Because the contributions from the electric double layer and the nondouble layer energy of adsorption are accounted for by the two integral terms in eq 1, γ_{jk} represents the interfacial tensions of the boundaries between the pure phases, that is, for a liquid without adsorbing solutes ($\sigma = 0$ and $\Gamma_m = 0$).

The third term in the right-hand side of eq 1 is the electrostatic contribution, which can be alternatively written (for $z:z$ electrolytes) as²¹

$$\begin{aligned} G_{\text{el}} &= \int_{\Sigma} dS \int_0^{\sigma} \varphi_s(\sigma) d\sigma = \\ &= \int_{\Sigma} \sigma \varphi dS - \int_{\Omega} [1/2 \epsilon |\nabla \varphi|^2 + \Pi(\varphi)] d\Omega \end{aligned} \quad (3)$$

where ϵ is the electric permittivity of the droplet, $\Pi = 2r^b kT [\cosh \beta \varphi - 1]$ is the osmotic pressure, r^b is the number density of ionic species in the bulk region, k is the Boltzmann constant, T is the absolute temperature, and $\beta = ze/kT$. The electrostatic potential φ satisfies the following Poisson–Boltzmann equation inside the droplet:

- (19) Marmur, A.; Krasovitski, B. *Langmuir* **2002**, *18*, 8919–8923.
 (20) Pompe, T.; Herminghaus, S. *Phys. Rev. Lett.* **2000**, *85*, 1930–1933.
 (21) Overbeek, J. T. G. *Colloids Surf.* **1990**, *51*, 61–75.
 (22) McCormack, D.; Carnie, S. L.; Chan, D. Y. C. *J. Colloid Interface Sci.* **1995**, *169*, 177–196.
 (23) Kralchevsky, P. A.; Danov, K. D.; Broze, G.; Mehreteab, A. *Langmuir* **1999**, *15*, 2351–2365.
 (24) Hachisu, S. *J. Colloid Interface Sci.* **1970**, *33*, 445–454.

$$\nabla^2 \varphi = (\kappa^2/\beta) \sinh \beta \varphi \quad (4)$$

where $\kappa^{-1} = (2n^b z^2 e^2 / \epsilon k T)^{-1/2}$ represents the Debye length.

For the CC case, the amount of adsorbed ions per unit surface area is uniform over each surface. If we assume that the chemical potential at the surface ($\bar{\mu}_m^s$) is the function of only Γ_m [i.e., $\bar{\mu}_m^s = \bar{\mu}_m^s(\Gamma_m)$], the chemical free energy per unit surface area is constant over each surface. If we omit G_{chem}^σ , there is no difference in the final result of the line tension. Even if we proceed with retaining G_{chem}^σ , it will be absorbed into the bulk part of the free energy (G_∞^σ ; defined later in eqs 7 and 8), which has no contribution to the excess free energy. For now, we omit G_{chem}^σ in the electrochemical free energy for the CC case; that is, $G^\sigma = G - G_{\text{chem}}^\sigma$, which becomes²²

$$G^\sigma = G_{\text{el}}^{\sigma,\varphi} = \int_\Sigma \sigma \varphi \, dS - \int_\Omega [1/2 \epsilon |\nabla \varphi|^2 + \Pi(\varphi)] \, d\Omega \quad (5)$$

Note that, for the sake of convenience, $G^\sigma = G - G_{\text{chem}}^\sigma$ is again called the electrochemical free energy.

For the CP case, if the equilibrium condition of $\mu_m^s = \mu_m^b$ is considered, $\bar{\mu}_m^s - \mu_m^s = -z_m e \varphi_s$ in eq 2 becomes constant. After substituting this into G_{chem}^σ and then by using $\sigma = \sum_m z_m e \Gamma_m$, we obtain the chemical free energy as $G_{\text{chem}}^\sigma = -\int_\Sigma \sigma \varphi \, dS$.^{21,22} Thus, the electrochemical free energy in this case ($G^\varphi = G_{\text{el}} + G_{\text{chem}}^\varphi$) becomes

$$G^\varphi = - \int_\Omega [1/2 \epsilon |\nabla \varphi|^2 + \Pi(\varphi)] \, d\Omega \quad (6)$$

In the CP case, the chemical free energy loss of the bulk electrolyte due to charge transfer to the surfaces is exactly balanced by the increase of the electrostatic free energy (see ref 25, p 398). This is analogous to the case of pure electrostatics in which the bulk electrolyte is the charge reservoir.²⁶ Note that the difference between G^σ and G^φ is that the surface-integral term in G^σ disappears in G^φ , which arises because G_{chem}^σ is omitted in G^φ .

We totally neglected the free energy contribution from the air phase ab initio. This can be justified as follows. The electric permittivity of the aqueous electrolyte solution is significantly greater than that of air. Thus, the contribution of the air phase to the first term in the volume integral in $G^{\sigma,\varphi}$ can be neglected. We assume here that the air–substrate interface is not charged. So, the surface-integral term in G^σ in the air phase is null. Last, the ion density in the air phase is negligible, so that the osmotic pressure term vanishes in the air phase.

Electrostatic Line Tension and Contact Angle

The electrostatic contribution to the line tension is composed of two parts. One arises from the local change of interfacial tension (due to the electrocapillary effect) by the excess electrostatic interaction in the TCL region. The other arises from the shape distortion from the straight interface. The latter contribution inevitably necessitates the analysis to find the interfacial shape, which is beyond the scope of the present investigation. As a first attempt to the theoretical modeling of the line tension in charge-related phenomena, it seems reasonable to consider the first part of the line tension. Thus, we assume a straight interface, which naturally leads to a wedgelike geometry.

(25) Hunter, R. J. *Foundations of Colloid Science*; Oxford University Press: New York, 1987; Vol. 1.

(26) Landau, L. D.; Lifshitz, E. M. *Electrodynamics of Continuous Media*; Pergamon Press: Sydney, 1960; p 32.

The electrochemical free energy (G^σ and G^φ) can be represented as the sum of the free energy of the system that would be obtained if there is no double layer interaction near the TCL ($G_\infty^{\sigma,\varphi}$, we call here the bulk part) and the remainder; that is,

$$G^{\sigma,\varphi} = G_\infty^{\sigma,\varphi} + \tau_{\text{el}}^{\sigma,\varphi} L \quad (7)$$

for each case. Here, L is the length of the contact line (i.e., the perimeter), which becomes $L = 2\pi R$ for an axisymmetric droplet having a base radius of R . The second term represents the contribution from the excess free energy due to the electrostatic effect (i.e., the electrostatic line tension τ_{el}). As mentioned in the Introduction, we omit the molecular contribution to the line tension because it is not considered in the present work.

The bulk part of the free energy ($G_\infty^{\sigma,\varphi}$) can be further decomposed into two contributions, which are associated with the droplet–substrate interface (S_{13}) and the droplet–air interface (S_{12}). Thus, for both the CC and the CP cases

$$G_\infty^{\sigma,\varphi} = g_1^{\sigma,\varphi} A_{13} + g_2^{\sigma,\varphi} A_{12} \quad (8)$$

For the CC and CP cases, the free energy per unit surface area far from the TCL in each surface ($g_j^{\sigma,\varphi}$, where $j = 1$ and 2 denote the values associated with S_{13} and S_{12} , respectively) becomes, from eqs 5 and 6,

$$g_j^\sigma = \sigma \varphi_{j\infty} - \frac{8n^b kT}{\kappa} \left[\cosh \frac{\beta \varphi_{j\infty}}{2} - 1 \right] \quad (9a)$$

$$g_j^\varphi = - \frac{8n^b kT}{\kappa} \left[\cosh \frac{\beta \varphi_{j\infty}}{2} - 1 \right] \quad (9b)$$

where $\varphi_{j\infty}$ represents the surface potential far from the TCL. The difference between g_j^σ and g_j^φ is again caused by omitting the chemical contribution for the CC case.

Next, we consider how the line tension contributes to the macroscopic energy balance. The total free energy of the system in eq 1 can be rewritten, by decomposing the electrochemical contribution as shown in eqs 7 and 8, as

$$G_{\text{tot}}^{\sigma,\varphi} = (\gamma_{12} + g_2^{\sigma,\varphi}) A_{12} + (\gamma_{13} + g_1^{\sigma,\varphi} - \gamma_{23}) A_{13} + 2\pi R \tau_{\text{el}}^{\sigma,\varphi}(\alpha) \quad (10)$$

Note that we left the line tension, which is often regarded as a constant, as a function of the contact angle (α). Applying the minimum free energy requirement of thermodynamics for equilibrium of an axisymmetric droplet, the following modified Young's equation is obtained:

$$\gamma_{12}' \cos \alpha = \gamma_{23} - \gamma_{13} - h_1^{\sigma,\varphi} - \frac{\tau_{\text{el}}^{\sigma,\varphi}}{R} - \frac{\partial \tau_{\text{el}}^{\sigma,\varphi}}{\partial R} \quad (11)$$

where $h_1^\varphi = g_1^\varphi$, $h_1^\sigma = g_1^\sigma + \sigma \varphi_0$, and φ_0 denotes the electrostatic potential at the TCL. The additional term $\sigma \varphi_0$ for the CC case originated from the change of the base area of the droplet and the consequent change of the total amount of surface charges at the droplet–substrate interface (see, for details, refs 16 and 17). Here, γ_{12}' is the modified interfacial tension due to the electrocapillary effect at the droplet–air interface, which becomes

$$\gamma_{12}' = \gamma_{12} - \frac{8n^b kT}{\kappa} \left[\cosh \frac{\beta \varphi_{j\infty}}{2} - 1 \right] \quad (12)$$

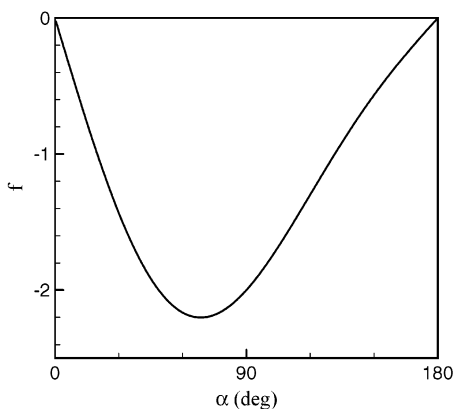


Figure 2. Function f .

at a far distance away from the TCL. The interfacial tension contributed by the curvature of S_{12} can be considered additionally in γ_{12} . The fifth term on the right-hand side of eq 11 represents, eventually, the contact angle dependence of the electrostatic line tension. The molecular counterpart of such a contact-angle-dependent contribution to Young's equation has been suggested by Marmur and Wolansky^{27–29} and Krotov and Rusanov.³⁰

The volume of a droplet (V_L) is related to the base radius and the contact angle as $V_L = (\pi R^3/3)(1 - \cos \alpha)^2(2 + \cos \alpha) \operatorname{cosec}^3 \alpha$ (see ref 25, p 300). By taking the derivative of both sides of the foregoing relation with respect to α , we obtain

$$\frac{\partial \alpha}{\partial R} = \frac{\cos \alpha + \cos^2 \alpha - 2}{R \tan(\alpha/2)} \equiv \frac{f(\alpha)}{R}$$

where

$$f(\alpha) = \frac{\cos \alpha + \cos^2 \alpha - 2}{\tan(\alpha/2)} \quad (13)$$

Figure 2 shows the function f . The function f always has a negative value, and $f=0$ at $\theta=0$ and 180° ; therefore, α decreases as R increases. Because $\partial \tau_{el}/\partial R = \partial \alpha/\partial R \times \partial \tau_{el}/\partial \alpha$, the modified Young's equation becomes

$$\gamma_{12}' \cos \alpha = \gamma_{23} - \gamma_{13} - h_1^{\sigma, \varphi} - \frac{1}{R} \left[\tau_{el}^{\sigma, \varphi} + f(\alpha) \frac{\partial \tau_{el}^{\sigma, \varphi}}{\partial \alpha} \right] \quad (14)$$

For a straight interface, the motion of the contact line induces translation of contact line (Figure 3b), rotation of the droplet–air interface (Figure 3c), and extension of the contact line (Figure 3d). In eq 14, $h_1^{\sigma, \varphi}$ corresponds to the free energy change due to the translation of the contact line (Figure 3b). That is, it is the electrostatic contribution to the wetting tension.¹⁶ The line-tension term τ_{el}/R represents the work done to increase the base radius (contact line; Figure 3d). As mentioned earlier, the line tension is often assumed to be constant. On the other hand, a certain extent of external work should be done to change the contact angle itself, overcoming the repulsive electrostatic interaction at the TCL. This part is represented in eq 14 as $f(\alpha)/R \times \partial \tau_{el}/\partial \alpha$ (see, for the molecular counterpart, refs 19 and 27–30).

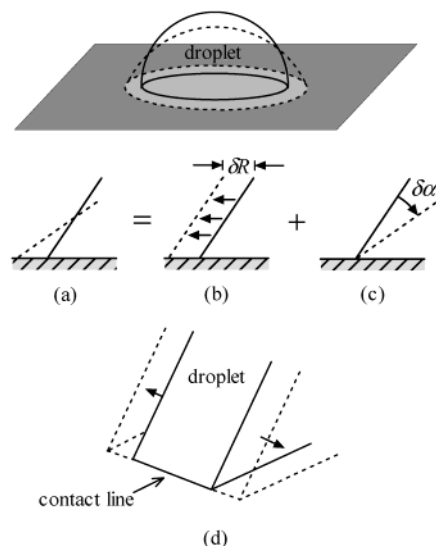


Figure 3. Decomposition of the contact-line motion. (a) Motion of contact line. (b) Translation in the radial direction. (c) Rotation. (d) Extension in the contact-line direction.

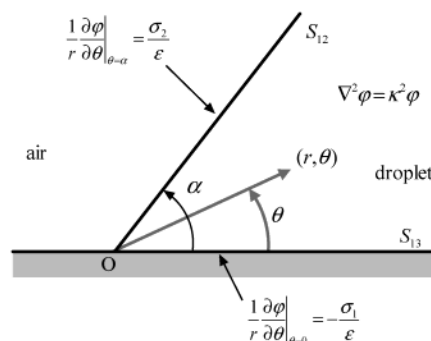


Figure 4. Domain of the analysis of the electrostatic field.

In the following section, the linearized Poisson–Boltzmann equation will be analyzed for the CC and the CP cases to determine τ_{el} and $\partial \tau_{el}/\partial \alpha$. Before proceeding, we linearized the electrochemical free energies as (see, for more details, appendix A)

$$G^\sigma = 1/2 \int_{\Sigma} \sigma \varphi \, dS \quad (15a)$$

$$G^\varphi = -1/2 \int_{\Sigma} \sigma \varphi \, dS \quad (15b)$$

As noted earlier, the difference between G^σ and G^φ arises because we omit G_{chem} in G^σ .

CC Case

Electrostatic Potential. As mentioned earlier, the shape of the edge of the liquid layer is modeled as wedgelike geometry (see Figure 4). A (r, θ) cylindrical coordinate system is introduced in which the origin is placed at the TCL.

The Poisson–Boltzmann equation can be rewritten in linearized form in the cylindrical coordinate system as

$$\nabla^2 \varphi = \frac{1}{r} \frac{\partial}{\partial r} \left(r \frac{\partial \varphi}{\partial r} \right) + \frac{1}{r^2} \frac{\partial^2 \varphi}{\partial \theta^2} = \kappa^2 \varphi \quad (16)$$

On the substrate surface, a constant charge density of σ_1 is assumed, which is written in the cylindrical coordinate system as

(27) Marmur, A. *J. Colloid Interface Sci.* **1997**, *186*, 462–466.

(28) Marmur, A. *Colloid Surf. A* **1998**, *136*, 81–88.

(29) Wolansky, G.; Marmur, A. *Langmuir* **1998**, *14*, 5292–5297.

(30) Krotov, V. V.; Rusanov, A. I. *Physicochemical Hydrodynamics of Capillary Systems*; Imperial College Press: London, 1999; p 16–19.

$$\frac{1}{r} \frac{\partial \varphi(\mathbf{r}, 0)}{\partial \theta} = -\frac{\sigma_1}{\epsilon} \quad (17)$$

At the droplet–air interface, it is assumed that there are electrical charges with the constant charge density σ_2 . Because the electric permittivity of aqueous electrolyte solution is much greater than that of air, the electric flux into (or from) the air phase can be neglected. Then, at the droplet–air interface, the following boundary condition can be applied:

$$\frac{1}{r} \frac{\partial \varphi(r, \alpha)}{\partial \theta} = \frac{\sigma_2}{\epsilon} \quad (18)$$

where α represents the wedge (contact) angle.

The solution for the CC case, in which the insulating condition is applied at the droplet–air interface (i.e., $\sigma_2 = 0$), was originally given by Fowkes and Hood³¹ by introducing the Kantorovich–Lebedev transform. Here, we extend the analysis to the case of arbitrary (but constant) charge density.

The transform and its inverse transform of Kantorovich–Lebedev are defined respectively as

$$\tilde{\varphi}(\theta, \lambda) = \int_0^\infty \varphi(r, \theta) K_{i\lambda}(\kappa r) \frac{dr}{r} \quad (19a)$$

$$\varphi(r, \theta) = \frac{2}{\pi^2} \int_0^\infty \tilde{\varphi}(\theta, \lambda) K_{i\lambda}(\kappa r) \lambda \sinh \pi \lambda \, d\lambda \quad (19b)$$

where $K_{i\lambda}(\kappa r)$ is the modified Bessel function^{32,33} and $i = (-1)^{1/2}$. Applying the Kantorovich–Lebedev transform to the linearized Poisson–Boltzmann equation, we obtain

$$\frac{\partial^2 \tilde{\varphi}}{\partial \theta^2} - \lambda^2 \tilde{\varphi} = 0 \quad (20)$$

The modified Bessel function $K_{i\lambda}(\kappa r)$ can be rewritten as $K_{i\lambda}(\kappa r) = \int_0^\infty e^{-\kappa r \cosh t} \cos \lambda t \, dt$ (ref 33, eq 9.6.24). Then, it becomes (ref 34, eq 3.981.3)

$$\int_0^\infty K_{i\lambda}(\kappa r) \, dr = \frac{1}{\kappa} \int_0^\infty \frac{\cos \lambda t}{\cosh t} \, dt = \frac{\pi}{2\kappa} \frac{1}{\cosh(\lambda\pi/2)} \quad (21)$$

By using the foregoing formula, the boundary conditions in eqs 17 and 18 are transformed respectively as $\partial \tilde{\varphi}(0, \lambda)/\partial \theta = -\pi \varphi_{1\infty} / [2 \cosh(\lambda\pi/2)]$ and $\partial \tilde{\varphi}(\alpha, \lambda)/\partial \theta = \pi \varphi_{2\infty} / [2 \cosh(\lambda\pi/2)]$, where $\varphi_{1\infty} = \sigma_1/(\epsilon\kappa)$ and $\varphi_{2\infty} = \sigma_2/(\epsilon\kappa)$ represent the electrostatic potential at the droplet–substrate and the droplet–air interfaces far from the TCL, respectively.

The solution of the transformed Poisson–Boltzmann equation (eq 20) can be written in the form of $\tilde{\varphi}(\theta, \lambda) = A_1(\lambda) \cosh \lambda(\theta - \alpha) + A_2(\lambda) \cosh \lambda\theta$. The unknown coefficients $A_1(\lambda)$ and $A_2(\lambda)$ are determined by using the transformed boundary conditions as $A_1(\lambda) = [\pi \varphi_{1\infty} / (2\lambda)] / [\sinh \lambda\alpha \cosh(\lambda\pi/2)]$ and $A_2(\lambda) = [\pi \varphi_{2\infty} / (2\lambda)] / [\sinh \lambda\alpha \cosh(\lambda\pi/2)]$. The resulting solution in λ space becomes

$$\tilde{\varphi}(\theta, \lambda) = \frac{\pi}{2\lambda \sinh \lambda\alpha \cosh(\lambda\pi/2)} \times \{ \varphi_{1\infty} \cosh \lambda(\theta - \alpha) + \varphi_{2\infty} \cosh \lambda\theta \}$$

Applying the inverse transform to the foregoing equation, one obtains the following solution

$$\varphi(r, \theta) = \frac{2}{\pi} \int_0^\infty \frac{\sinh(\lambda\pi/2)}{\sinh \lambda\alpha} \{ \varphi_{1\infty} \cosh \lambda(\theta - \alpha) + \varphi_{2\infty} \cosh \lambda\theta \} K_{i\lambda}(\kappa r) \, d\lambda \quad (22)$$

Line Tension. If we rewrite the linearized electrochemical free energy for the present CC case shown in eq 15a, it becomes

$$G^\sigma = \frac{L}{2} \{ \sigma_1 \int_0^\infty \varphi(r, 0) \, dr + \sigma_2 \int_0^\infty \varphi(r, \alpha) \, dr \} \quad (23)$$

where $L = 2\pi R$ for an axisymmetric droplet. Substituting φ in eq 22 into eq 23, we obtain

$$G^\sigma = \frac{\epsilon\kappa L}{\pi} \left\{ \varphi_{1\infty} \int_0^\infty \int_0^\infty \frac{\sinh(\lambda\pi/2)}{\sinh \lambda\alpha} \{ \varphi_{1\infty} \cosh \lambda\alpha + \varphi_{2\infty} \} K_{i\lambda}(\kappa r) \, dr \, d\lambda + \varphi_{2\infty} \int_0^\infty \int_0^\infty \frac{\sinh(\lambda\pi/2)}{\sinh \lambda\alpha} \{ \varphi_{1\infty} + \varphi_{2\infty} \cosh \lambda\alpha \} K_{i\lambda}(\kappa r) \, dr \, d\lambda \right\}$$

By using eq 21, we can show, without difficulty, that the foregoing relation is changed to

$$G^\sigma = \frac{\epsilon L}{2} \int_0^\infty \frac{\sinh(\lambda\pi/2)}{\cosh(\lambda\pi/2) \sinh \lambda\alpha} \{ \varphi_{1\infty}^2 \cosh \lambda\alpha + \varphi_{2\infty}^2 \cosh \lambda\alpha + 2\varphi_{1\infty}\varphi_{2\infty} \} \, d\lambda$$

From eq 7, the electrostatic contribution to the excess free energy (i.e, the electrostatic line tension) can be obtained by using

$$\tau_{el}^\sigma = \frac{G^\sigma - G_\infty^\sigma}{L}$$

To obtain the line tension, the bulk free energy of the electrical double layer (G_{el}^σ) should be subtracted from G^σ , where G_∞^σ becomes from eq 15a

$$G_\infty^\sigma = \frac{\epsilon L}{2} \int_0^\infty (\varphi_{1\infty}^2 + \varphi_{2\infty}^2) \, d\lambda$$

Then, the excess free energy in the present CC condition becomes

$$\tau_{el}^\sigma(\alpha) = \frac{\epsilon}{2} \int_0^\infty \left\{ \frac{\sinh(\lambda\pi/2)}{\cosh(\lambda\pi/2) \sinh \lambda\alpha} \{ \varphi_{1\infty}^2 \cosh \lambda\alpha + \varphi_{2\infty}^2 \cosh \lambda\alpha + 2\varphi_{1\infty}\varphi_{2\infty} \} - (\varphi_{1\infty}^2 + \varphi_{2\infty}^2) \right\} \, d\lambda$$

After changing the variable as $\lambda = 2\omega$ and careful manipulation of the formulas, the foregoing equation can be rearranged as follows:

$$\tau_{el}^\sigma(\alpha) = \epsilon (\varphi_{1\infty}^2 + \varphi_{2\infty}^2) M_1(\alpha) - \epsilon (\varphi_{1\infty} - \varphi_{2\infty})^2 M_2(\alpha) \quad (24)$$

where $M_1 = \int_0^\infty (\tanh \omega\pi / \tanh \omega\alpha - 1) \, d\omega$ and $M_2 =$

(31) Fowkes, N. D.; Hood, M. J. *J. Mech. Appl. Math.* **1998**, *51*, 553–561.

(32) Arfken, G. *Mathematical Methods for Physicists*, 3rd ed.; Academic Press: London, 1985; p 610–616.

(33) Abramowitz, M.; Stegun, I. A. *Handbook of Mathematical Functions*; Dover Publications: New York, 1972.

(34) Gradshteyn, I. S.; Ryzhik, I. M. *Table of Integrals, Series, and Products*; Academic Press: London, 1965.

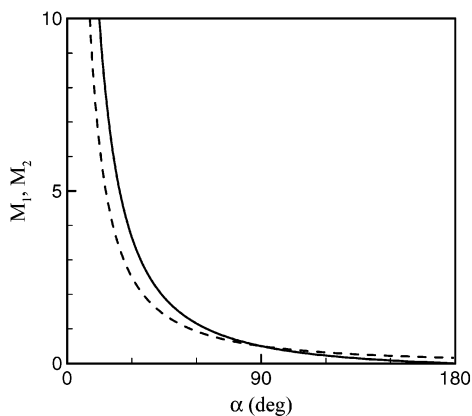


Figure 5. Solid line, M_1 ; dashed line, M_2 .

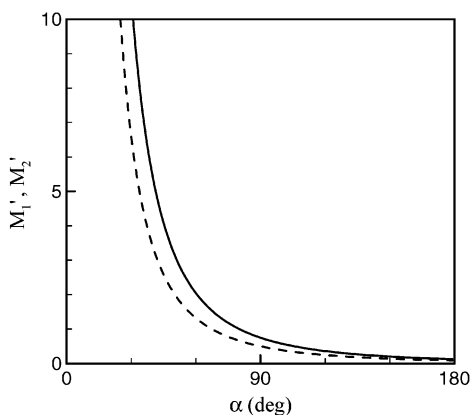


Figure 6. Solid line, M_1' ; dashed line, M_2' .

$\int_0^\infty (\tanh \omega\pi/\sinh 2\omega\alpha - 1) d\omega$. Duplantier³⁵ has obtained the excess free energy of the wedge-shaped singularity of a membrane for both the CC and the CP cases (but having identical charge density and potential for the two surfaces) with a different approach. When $\varphi_{1\infty} = \varphi_{2\infty}$, the second term vanishes and the line tension becomes $2\epsilon\varphi_{1\infty}^2 M_1(\alpha)$, which is consistent with Duplantier's result for the present case. It should be noted, however, that in most circumstances the surface charge density of the droplet-substrate interface is different from that of the droplet-air interface, as postulated in the present investigation.

The gradient of the line tension with respect to α (i.e., $\partial\tau_{el}/\partial\alpha$), which appears in the modified Young's equation (eq 14), can be obtained from eq 24 as

$$\frac{\partial\tau_{el}^\sigma}{\partial\alpha} = -\epsilon(\varphi_{1\infty}^2 + \varphi_{2\infty}^2)M_1'(\alpha) + \epsilon(\varphi_{1\infty} - \varphi_{2\infty})^2 M_2'(\alpha) \quad (25)$$

where $M_1' = \int_0^\infty \omega \tanh \omega\pi/\sinh^2 \omega\alpha d\omega$ and $M_2' = \int_0^\infty 2\omega \tanh \omega\pi/(\sinh 2\omega\alpha \tanh 2\omega\alpha) d\omega$.

It is noted that, when $\alpha = \pi$, $M_1(\alpha)$; that is, the line tension becomes 0. This is reasonable considering that $\alpha = \pi$ and $\varphi_{1\infty} = \varphi_{2\infty}$ mean the case of a flat electrical double layer. As shown in Figures 5 and 6, the functions M_1 , M_2 , M_1' , and M_2' are positive for all values of α and monotonically increase as α decreases. Eventually, all the functions M_1 , M_2 , M_1' , and M_2' diverge as $\alpha \rightarrow 0$. This results because, when $\alpha \rightarrow 0$, not only the electrostatic potential itself increases near the TCL but also the area of the high potential region is broadened. The physical consequence of that can be described as follows:

Consider a special case in which the two surfaces have identical surface charge densities; that is, $\varphi_{1\infty} = \varphi_{2\infty}$. Then, it becomes

$$\tau_{el}^\sigma = 2\epsilon\varphi_{1\infty}^2 M_1(\alpha)$$

$$\frac{\partial\tau_{el}^\sigma}{\partial\alpha} = -2\epsilon\varphi_{1\infty}^2 M_1'(\alpha)$$

and thus

$$\tau_{el}^\sigma + f \frac{\partial\tau_{el}^\sigma}{\partial\alpha} = 2\epsilon\varphi_{1\infty}^2 (M_1 - fM_1')$$

Note that f is negative for $\alpha < \pi$ (see Figure 2) and both M_1 and M_1' are always positive; consequently, the above equation is always positive for $\alpha < \pi$ (provided $\varphi_{1\infty} = \varphi_{2\infty}$). It follows, therefore, that the term in the bracket in the modified Young's equation (eq 14) tends to oppose the decrease of the contact angle. As a result, the contact angles predicted with considering the line-tension effect will give higher values than those predicted without considering the line-tension effect. The reduction of the contact angle will increase the electrostatic potential near the TCL, which necessitates (as explained earlier) the *additional* increase of the free energy of the system by the external work (see Figure 3c). In addition, the decrease of the contact angle requires an extension of the contact line, which also requires an *additional* increase of the free energy as schematically shown in Figure 3d.

The divergence of M_1 and M_1' as $\alpha \rightarrow 0$ literally means that the perfect wetting of the liquid droplet is not possible as a result of the line-tension effect. It is evidently not true for the actual systems. In actual situations, the liquid surface in close to the TCL will deform (due to the action of the disjoining pressure) as the contact angle decreases, as noted by de Gennes (see Figure 4b of ref 36). Consequently, the validity of the straight-line assumption for the liquid surface of the present investigation will be degraded. At present, such large values of M_1 and M_1' (in this special case of $\varphi_{1\infty} = \varphi_{2\infty}$) should be interpreted as the resisting role of the line tension to the reduction of the contact angle with keeping the interface straight.

When α is smaller (greater) than $\pi/2$, M_1 is greater (smaller) than M_2 for all α . Let us consider the case of $M_1(\pi/2) = M_2(\pi/2) = 1/2$. Then, from eq 24, the line tension becomes

$$\tau_{el}^\sigma(\pi/2) = \frac{\epsilon}{2}(\varphi_{1\infty}^2 + \varphi_{2\infty}^2) - \frac{\epsilon}{2}(\varphi_{1\infty} - \varphi_{2\infty})^2 = \epsilon\varphi_{1\infty}\varphi_{2\infty} = \frac{\sigma_1\sigma_2}{\epsilon\kappa^2}$$

When $\alpha = \pi/2$, the sign of the line tension becomes positive or negative depending on the signs of the surface charge. Although the detailed condition of sign change is not clearly shown here, it is evident that the line tension can have either a positive or a negative value.

CP Case

In this case, the electrostatic potentials at the droplet-substrate and the droplet-air interfaces are maintained with constant values as $\varphi(r, 0) = \varphi_1$ and $\varphi(r, \alpha) = \varphi_2$. The overall procedure to obtain the potential distribution and the line tension is similar to the earlier CC case. The resulting electrostatic potential and the line tension

(35) Duplantier, B. *Phys. Rev. Lett.* **1991**, *66*, 1555–1558.

(36) de Gennes, P. G. *Rev. Mod. Phys.* **1985**, *57*, 827–863.

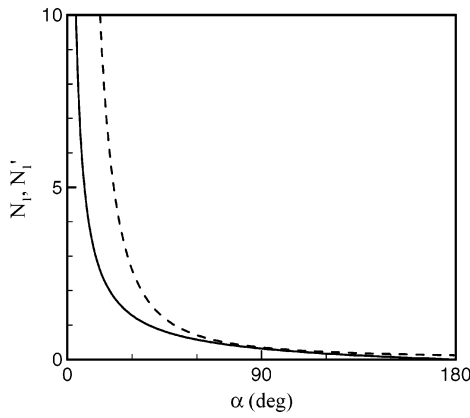


Figure 7. Solid line, N_1 ; dashed line, N_1' .

become (see appendix B)

$$\varphi(r, \theta) = \frac{2}{\pi} \int_0^\infty \frac{\cosh(\lambda\pi/2)}{\sinh \lambda\alpha} \{-\varphi_1 \sinh \lambda(\theta - \alpha) + \varphi_2 \sinh \lambda\theta\} K_{i\lambda}(\kappa r) d\lambda \quad (26)$$

$$\tau_{el}^\varphi(\alpha) = \epsilon(\varphi_1^2 + \varphi_2^2)N_1(\alpha) - \epsilon(\varphi_1 - \varphi_2)^2N_2(\alpha) \quad (27)$$

where $N_1 = \int_0^\infty (1 - \tanh \omega\alpha / \tanh \omega\pi) d\omega$ and $N_2 = \int_0^\infty (\tanh \omega\pi / \sinh 2\omega\alpha)^{-1} d\omega$.

The function N_2 diverges irrespective of α . So, the line tension has a bounded value only when $\varphi_1 = \varphi_2$.³⁷ This condition makes the second term in eq 27 vanish, and the line tension becomes

$$\tau_{el}^\varphi = 2\epsilon\varphi_1^2N_1(\alpha) \quad (28)$$

which is consistent with Duplantier's result for the CP case.³⁵ The gradient of the line tension with respect to α can be obtained from eq 28 as

$$\frac{\partial \tau_{el}^\varphi}{\partial \alpha} = -2\epsilon\varphi_1^2N_1'(\alpha) \quad (29)$$

where $N_1' = \int_0^\infty \omega(\cosh^2 \omega\alpha \tanh \omega\pi)^{-1} d\omega$.

As shown in Figure 7, the functions N_1 and N_1' monotonically increases as α decreases and always have positive values. From eqs 28 and 29, it becomes

$$\tau_{el}^\varphi + f \frac{\partial \tau_{el}^\varphi}{\partial \alpha} = 2\epsilon\varphi_1^2(N_1 - fN_1')$$

The function f is negative for $\alpha < \pi$. Thus, in this case, the line-tension term in the modified Young's equation is also negative for $\alpha < \pi$. Like the CC case, this means that the line tension has an opposing role to the reduction of the contact angle for $\alpha < \pi$. The divergence of N_1 and N_1' can be understood in a fashion similar to those of the functions M_1, M_2, M_1' and M_2' of the CC case.

Note that, for $\alpha = \pi, N_1(\alpha) = 0$. Therefore, the line tension becomes 0. This is reasonable considering that $\alpha = \pi$ and $\varphi_1 = \varphi_2$ also mean the case of a flat electrical double layer.

(37) Note that the line tension is proportional to the integral of the induced (or excess) surface charge (see eqs 7 and 15b). The gradient of electrostatic potential becomes extremely large near the TCL due to the abrupt change of the electrostatic potential at the two surfaces. This will induce a large magnitude of surface charge around the TCL.

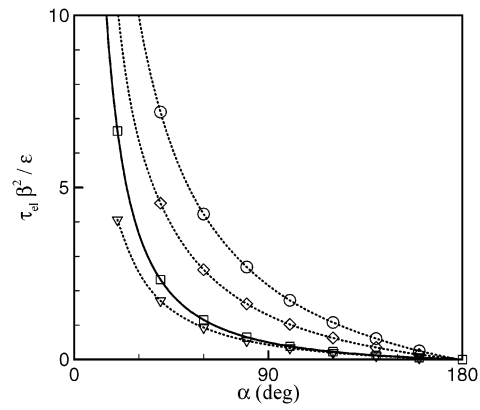


Figure 8. Calculated line tension. Solid line is for the analytical solution of the linear theory. Symbols indicate the numerical results. Squares are for the linearized equation with $\beta\sigma_1/(\epsilon\kappa) = 1$. Triangles, diamonds, and circles are for the nonlinear equation with $\beta\sigma_1/(\epsilon\kappa) = 1, 2,$ and 3 , respectively.

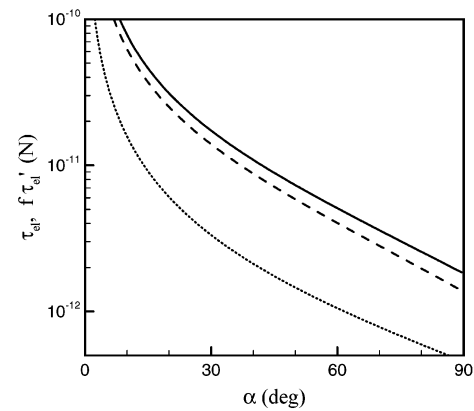


Figure 9. Sample calculation of the line tension for $\beta\sigma_1/(\epsilon\kappa) = 1$ ($\varphi_{1\infty} = 25.7$ mV by the linear theory). Dotted, dashed, and solid lines correspond to $\tau_{el}, f\partial\tau_{el}/\partial\alpha,$ and $\tau_{el} + f\partial\tau_{el}/\partial\alpha$, respectively.

Numerical Validation and Sample Calculation

For verification of the linear theory, the line tension is obtained numerically for the CC case. To analyze the electrostatic field, a numerical method based on the calculus of variation is used. The details of the numerical method are described in ref 17. After analyzing the electrostatic field, the free energy can be calculated by using eq 5 or its linearized version of eq 15a. The calculation is performed for three dimensionless surface charge densities of $\beta\sigma_1/(\epsilon\kappa) = \beta\sigma_2/(\epsilon\kappa) = 1, 2,$ and 3 . The conditions of $\beta\sigma_1/(\epsilon\kappa) = 1, 2,$ and 3 correspond to the surface potential values ($\varphi_{1\infty}$) of 25.7, 51.4, and 77.1 mV, respectively, for the linear theory. For the nonlinear theory, they become 24.7, 45.3, and 61.4 mV, respectively.

The numerical results on the line tension of the linearized Poisson–Boltzmann equation (squares in Figure 8) are compared with the linear theory of eq 24 (solid line) for various contact angles. As shown in the figure, the numerical results obtained by using the linearized Poisson–Boltzmann equation agree with the analytical result very well. For $\beta\sigma_1/(\epsilon\kappa) = 1$, the nonlinear analysis gives smaller τ_{el} than the linear analysis for all contact angles; for smaller contact angles, the deviation between the linear and the nonlinear results becomes greater as the contact angle decreases.

The results of the sample calculation for $\tau_{el}, f\partial\tau_{el}/\partial\alpha,$ and $\tau_{el} + f\partial\tau_{el}/\partial\alpha$ are shown in Figure 9. The case of rather small surface charge (potential) of $\beta\sigma_1/(\epsilon\kappa) = \beta\sigma_2/(\epsilon\kappa) = 1$

($\varphi_{1\infty} = \varphi_{2\infty} = 25.7$ mV) is chosen, considering the validity of the linear theory. For contact angles smaller than about 13° , the line tension itself is greater than $\tau_{el} = 2 \times 10^{-11}$ N. When the contact angle is further decreased, τ_{el} sharply increases in proportion to the surface potential value. The surface potential normally has greater values than 25.7 mV.

According to the recent measurement of the molecular contribution, $\tau = 1.6 \times 10^{-11}$ N for the decane droplet–water–air system,⁴ and $10^{-11} < \tau < 10^{-10}$ N for the hexaethylene glycol droplet (surrounded by air) on a silicon wafer where a thin line is printed by perfluorinated alkylsilanes.²⁰ It can be concluded, therefore, that the magnitude of the electrostatic contribution is at least comparable to the molecular contribution. For a higher surface charge density, it can have potentially a much greater value than that of the molecular contribution.

Conclusion

We obtained an analytical solution of the linearized Poisson–Boltzmann equation around a wedge-shaped geometry with respect to the constant surface charge and the constant surface potential conditions, respectively.

Comprehensive analytical formulas of the line tension and its gradient with respect to the contact angle for both conditions are obtained in eqs 24, 25, 28, and 29. In the CP case, however, the line tension has a bounded value only when the two surface potentials have the same values. It is demonstrated that the line tension has either a positive or a negative value for the CC condition depending on the values of the surface charge density, while under the CP condition it should always have a positive value.

The Poisson–Boltzmann equation is solved numerically to verify the analytical results. Also, it is demonstrated that the line tension has a magnitude comparable to that of the molecular contribution. In the case of higher surface potential or surface charge density, it can have a much greater value than that of the molecular contribution.

We assume here that the droplet surface maintains the straight profile. This assumption will lose its validity especially for small contact angles. A more correct assessment of the line-tension effect on the wetting problem may require consideration for the interfacial deformation (in a fashion similar to the work by Denkov et al.),¹⁸ which will be a subject to be pursued in the future investigation.

Acknowledgment. The present investigation was supported by the Brain Korea 21 Program in 2002 and by the Pohang Steel Company (POSCO) Technology Development Fund in 2002 (Contract No. 1UD02013) administered by the Pohang University of Science and Technology. I.S.K. was also supported by a grant from the Korea Science and Engineering Foundation (KOSEF; Contract No. R01-2001-00410). The authors deeply appreciate the comments of reviewers, which have been instrumental for the improvement of the revised manuscript.

Appendix A: Derivation of Equation 15

If we expand the cosine hyperbolic term in the free energy of eq 5, by using the Taylor series, we obtain

$$G^s = \int_{\Sigma} \sigma \varphi \, dS - \frac{1}{2} \int_{\Omega} \epsilon [|\nabla \varphi|^2 + \kappa^2 \varphi^2] \, d\Omega \quad (\text{A1})$$

Then, by using the linearized Poisson–Boltzmann equation of $\nabla^2 \varphi = \kappa^2 \varphi$ and a vector identity of

$$\nabla \cdot (\varphi \nabla \varphi) = |\nabla \varphi|^2 + \varphi \nabla^2 \varphi \quad (\text{A2})$$

eq A1 becomes

$$G^s = \int_{\Sigma} \sigma \varphi \, dS - \frac{1}{2} \int_{\Omega} \epsilon \nabla \cdot (\varphi \nabla \varphi) \, d\Omega \quad (\text{A3})$$

The volume integral in eq A3 can be transformed to the surface integral by using the divergence theorem of

$$\int_{\Omega} \epsilon \nabla \cdot (\varphi \nabla \varphi) \, d\Omega = \int_{\Sigma} \varphi (\epsilon \mathbf{n} \cdot \nabla \varphi) \, dS = \int_{\Sigma} \sigma \varphi \, dS \quad (\text{A4})$$

Then, it becomes eq 15a, as follows:

$$G^s = \int_{\Sigma} \sigma \varphi \, dS - \frac{1}{2} \int_{\Sigma} \sigma \varphi \, dS = \frac{1}{2} \int_{\Sigma} \sigma \varphi \, dS \quad (\text{A5})$$

For the CP case, the first term in eqs A1 and A5 is canceled by the chemical contribution G_{chem} , which is omitted in G^s ; therefore, we obtain eq 15b.

Appendix B: Electrostatic Potential and Line Tension for the CP Case

Electrostatic Potential. For the time being, we take arbitrary values for the surface potentials of φ_1 and φ_2 , respectively. The CP boundary conditions at both interfaces are written as

$$\varphi(r, 0) = \varphi_1 \quad (\text{B1a})$$

$$\varphi(r, \alpha) = \varphi_2 \quad (\text{B1b})$$

The following relation holds for the integral of the modified Bessel function $K_{\lambda}(\kappa r)$ (see appendix C):

$$\int_0^{\infty} \frac{K_{\lambda}(\kappa r)}{r} \, dr = \frac{\pi}{2\lambda} \frac{1}{\sinh(\lambda\pi/2)} \quad (\text{B2})$$

By using eqs 19a and B2, the boundary conditions in eqs B1a and B1b are transformed respectively as

$$\tilde{\varphi}(0, \lambda) = \frac{\pi}{2\lambda} \frac{\varphi_1}{\sinh(\lambda\pi/2)} \quad (\text{B3a})$$

$$\tilde{\varphi}(\alpha, \lambda) = \frac{\pi}{2\lambda} \frac{\varphi_2}{\sinh(\lambda\pi/2)} \quad (\text{B3b})$$

The solution of eq 20 can be written in the form of $\tilde{\varphi}(\theta, \lambda) = B_1(\lambda) \sinh \lambda(\theta - \alpha) + B_2(\lambda) \sinh \lambda\theta$. The unknown coefficients $B_1(\lambda)$ and $B_2(\lambda)$ are determined by using the transformed boundary conditions in eq B3 as $B_1(\lambda) = -[\pi\varphi_1/(2\lambda)]/[\sinh \lambda\alpha \sinh(\lambda\pi/2)]$ and $B_2(\lambda) = [\pi\varphi_2/(2\lambda)]/[\sinh \lambda\alpha \sinh(\lambda\pi/2)]$, respectively. The resulting solution in λ space becomes

$$\tilde{\varphi}(\theta, \lambda) = \frac{\pi}{2\lambda \sinh \lambda\alpha \sinh(\lambda\pi/2)} \{-\varphi_1 \sinh \lambda(\theta - \alpha) + \varphi_2 \sinh \lambda\theta\}$$

Applying the inverse Kantorovich–Lebedev transform to the foregoing equation, one obtains the following solution

$$\varphi(r, \theta) = \frac{2}{\pi} \int_0^{\infty} \frac{\cosh(\lambda\pi/2)}{\sinh \lambda\alpha} \{-\varphi_1 \sinh \lambda(\theta - \alpha) + \varphi_2 \sinh \lambda\theta\} K_{\lambda}(\kappa r) \, d\lambda \quad (\text{B4})$$

Line Tension. If we rewrite the free energy for the CP case (eq 15b), it becomes

$$G^\varphi = \frac{L}{2} \left\{ \varphi_1 \int_0^\infty \frac{\partial \varphi(r, 0)}{\partial r} dr - \varphi_2 \int_0^\infty \frac{\partial \varphi(r, \alpha)}{\partial r} dr \right\}$$

Substituting eq B4 into the foregoing equation, we obtain

$$G^\varphi = \frac{\epsilon L}{\pi} \left\{ \varphi_1 \int_0^\infty \int_0^\infty \frac{\cosh(\lambda\pi/2)}{\sinh \lambda\alpha} \{-\varphi_1 \cosh \lambda\alpha + \varphi_2\} \frac{K_{i\lambda}(\kappa r)}{r} dr d\lambda - \varphi_2 \int_0^\infty \int_0^\infty \frac{\cosh(\lambda\pi/2)}{\sinh \lambda\alpha} \{-\varphi_1 + \varphi_2 \cosh \lambda\alpha\} \frac{K_{i\lambda}(\kappa r)}{r} dr d\lambda \right\}$$

By using eq B2, it can be shown without difficulty that the foregoing relation becomes

$$G^\varphi = \frac{\epsilon L}{2} \int_0^\infty \left\{ \frac{\cosh(\lambda\pi/2)}{\sinh(\lambda\pi/2) \sinh \lambda\alpha} \{-\varphi_1^2 \cosh \lambda\alpha - \varphi_2^2 \cosh \lambda\alpha + 2\varphi_1\varphi_2\} \right\} d\lambda$$

The bulk free energy of the electrical double layer [$G_\infty^\varphi = (-\epsilon L/2) \int_0^\infty (\varphi_1^2 + \varphi_2^2) d\lambda$] is subtracted to obtain the excess free energy. Then, the line tension in the present case ($\tau_{el}^\varphi = [G^\varphi - G_\infty^\varphi]/L$) becomes

$$\tau_{el}^\varphi(\alpha) = \frac{\epsilon}{2} \int_0^\infty \left\{ \frac{\cosh(\lambda\pi/2)}{\sinh(\lambda\pi/2) \sinh \lambda\alpha} \{-\varphi_1^2 \cosh \lambda\alpha - \varphi_2^2 \cosh \lambda\alpha + 2\varphi_1\varphi_2\} + (\varphi_1^2 + \varphi_2^2) \right\} d\lambda$$

After changing the variable as $\lambda = 2\omega$ and careful manipulation of the formulas, the foregoing equation can be rearranged as follows:

$$\tau_{el}^\varphi(\alpha) = \epsilon(\varphi_1^2 + \varphi_2^2)N_1(\alpha) - \epsilon(\varphi_1 - \varphi_2)^2N_2(\alpha) \quad (B5)$$

where $N_1 = \int_0^\infty (1 - \tanh \omega\alpha/\tanh \omega\pi) d\omega$ and $N_2 = \int_0^\infty (\tanh \omega\pi/\sinh 2\omega\alpha)^{-1} d\omega$.

Appendix C: Derivation of Equation B2

The modified Bessel function $K_{i\lambda}(\kappa r)$ can be rewritten as (ref 33, eq 9.6.22)

$$K_{i\lambda}(\kappa r) = \frac{\Gamma(i\lambda + 1/2)(2r)^{i\lambda}}{\pi^{1/2}\kappa^{i\lambda}} \int_0^\infty \frac{\cos \kappa t}{(t^2 + r^2)^{i\lambda + (1/2)}} dt$$

where Γ represents the gamma function. Because $\int_0^\infty t^{i\lambda-1}/(1+r^2)^{i\lambda+1/2} dr = 1/2[\Gamma(i\lambda/2) \Gamma(i\lambda/2 + 1/2)]/\Gamma(i\lambda + 1/2)$ (ref 34, eq 3.251.2), it becomes

$$\int_0^\infty \frac{K_{i\lambda}(\kappa r)}{r} dr = \frac{2^{i\lambda-1}\Gamma(i\lambda/2) \Gamma(i\lambda/2 + 1/2)}{\pi^{1/2}\kappa^{i\lambda}} \int_0^\infty \frac{\cos \kappa t}{t^{i\lambda+1}} dt$$

By using $\Gamma(i\lambda/2) \Gamma(i\lambda + 1/2) = \pi^{1/2}2^{-(i\lambda-1)}\Gamma(i\lambda)$ (ref 33, eq 6.1.18), the foregoing equation is changed to

$$\int_0^\infty \frac{K_{i\lambda}(\kappa r)}{r} dr = \frac{\Gamma(i\lambda)}{\kappa^{i\lambda}} \int_0^\infty \frac{\cos \kappa t}{t^{i\lambda+1}} dt$$

$\int_0^\infty \cos \kappa t/t^{i\lambda+1} dt = -\pi\kappa^{i\lambda}/[2i \sinh(\lambda\pi/2)\Gamma(i\lambda + 1)]$ (ref 34, eq 3.761.9) and $\Gamma(i\lambda + 1) = i\lambda\Gamma(i\lambda)$ (ref 33, eq 6.1.15), and, thus, it becomes

$$\int_0^\infty \frac{K_{i\lambda}(\kappa r)}{r} dr = \frac{\pi}{2\lambda} \frac{1}{\sinh(\lambda\pi/2)}$$